



QCD factorization of the four-lepton decay $B^- \rightarrow \ell \bar{\nu}_\ell \ell^{(\prime)} \bar{\ell}^{(\prime)}$

Martin Beneke¹, Philipp Böer^{1,a}, Panagiotis Rigatos¹, K. Keri Vos^{2,3}

¹ Physik Department T31, Technische Universität München, James-Frank-Straße 1, 85748 Garching, Germany

² Gravitational Waves and Fundamental Physics (GWFP), Maastricht University, Duboisdomein 30, 6229 GT Maastricht, The Netherlands

³ Nikhef, Science Park 105, 1098 XG Amsterdam, The Netherlands

Received: 26 February 2021 / Accepted: 25 June 2021 / Published online: 21 July 2021

© The Author(s) 2021

Abstract Motivated by the first search for the rare charged-current B decay to four leptons, $\ell \bar{\nu}_\ell \ell^{(\prime)} \bar{\ell}^{(\prime)}$, we calculate the decay amplitude with factorization methods. We obtain the $B \rightarrow \gamma^*$ form factors, which depend on the invariant masses of the two lepton pairs, at leading power in an expansion in Λ_{QCD}/m_b to next-to-leading order in α_s , and at $\mathcal{O}(\alpha_s^0)$ at next-to-leading power. Our calculations predict branching fractions of a few times 10^{-8} in the $\ell^{(\prime)} \bar{\ell}^{(\prime)}$ mass-squared bin up to $q^2 = 1 \text{ GeV}^2$ with $n_{+q} > 3 \text{ GeV}$. The branching fraction rapidly drops with increasing q^2 . An important further motivation for this investigation has been to explore the sensitivity of the decay rate to the inverse moment λ_B of the leading-twist B meson light-cone distribution amplitude. We find that in the small- q^2 bin, the sensitivity to λ_B is almost comparable to $B^- \rightarrow \ell^- \bar{\nu}_\ell \gamma$ when λ_B is small, but with an added uncertainty from the light-meson intermediate resonance contribution. The sensitivity degrades with larger q^2 .

1 Introduction

The radiative decay $B^- \rightarrow \ell^- \bar{\nu}_\ell \gamma$ has been extensively studied in the context of QCD factorization (QCDF) [1–5] when the energy of the photon E_γ is large compared to the scale of the strong interaction Λ_{QCD} . At leading power in a simultaneous expansion in $\Lambda_{\text{QCD}}/E_\gamma$ and Λ_{QCD}/m_b , and at leading order (LO) in the strong coupling α_s , the relevant $B \rightarrow \gamma$ transition form factor can be expressed in terms of only two hadronic parameters: the accurately known B meson decay constant f_B , and the poorly constrained first inverse moment $1/\lambda_B = \int_0^\infty d\omega \phi_+^B(\omega)/\omega$ of $\phi_+^B(\omega)$, the leading-twist B meson light-cone distribution amplitude (LCDA). This hadronic parameter was introduced in the theoretical description of charmless hadronic decays [6] and appears in the QCD calculation of almost any other exclusive B decay

to light particles. The radiative decay $B^- \rightarrow \ell^- \bar{\nu}_\ell \gamma$ has been advocated as a means to determine λ_B from data [5]. First significant measurements can be expected from the BELLE II experiment (see [7] for the most recent BELLE result).

This strategy is difficult to implement in the hadronic B experiment LHCb, since the photon in the radiative decay cannot be easily reconstructed. In this paper we investigate whether the four-lepton decay $B^- \rightarrow \ell \bar{\nu}_\ell \gamma^* \rightarrow \ell \bar{\nu}_\ell \ell^{(\prime)} \bar{\ell}^{(\prime)}$, in which the real photon is replaced by a virtual one, which decays into a lepton-antilepton pair ($\ell, \ell' = e, \mu$), retains sensitivity to λ_B , and hence could provide an alternative measurement. We focus on the kinematic region, where the γ^* , respectively the lepton pair, has large energy but small invariant mass $q^2 \lesssim 6 \text{ GeV}^2$.¹ The four-lepton decays have not been observed up to now, but the LHCb experiment [8] established an upper bound of $\text{Br}(B^+ \rightarrow \mu^+ \bar{\nu}_\mu \mu^- \mu^+) < 1.6 \cdot 10^{-8}$ on the branching fraction of the muonic mode under the assumption that the smaller of the two possible $\mu^+ \mu^-$ invariant masses is below 980 MeV, which is close to, in fact somewhat below, theoretical expectations [9, 10].

The factorization theorem for the $B \rightarrow \gamma$ form factors in the regime where the photon is energetic, $n_{+q} = 2E_\gamma \gg \Lambda_{\text{QCD}}$, has been established long ago [3, 4]. Its generalization to $B \rightarrow \gamma^*$ form factors is straightforward, when q^2 is away from light-meson resonances. The present treatment follows the strategy applied to $B^- \rightarrow \ell^- \bar{\nu}_\ell \gamma$ [5] and $B_s \rightarrow \mu^+ \mu^- \gamma$ [11] – we compute the form factor in QCD factorization at leading power (LP) including $\mathcal{O}(\alpha_s)$ QCD corrections, and include next-to-leading power (NLP) corrections at $\mathcal{O}(\alpha_s^0)$. The light-meson resonance contribution is included in the same fashion as for the “type-B” contribution to $B_s \rightarrow \mu^+ \mu^- \gamma$ [11]. Since the four-lepton final state is produced from a virtual W boson and photon, an extension of previous calculations is required to $B \rightarrow \gamma^*$ form factors

¹ In case of identical lepton flavours $\ell = \ell'$, the identification of the virtual photon with a lepton-antilepton pair is not unique, see later discussion.

^a e-mail: philipp.boer@tum.de (corresponding author)

that depend on two non-vanishing virtualities. We note that a previous computation [12] of these $B \rightarrow \gamma^*$ form factors includes either *only* the resonance contribution at small q^2 , or employs QCD sum rules that apply only to large $q^2 \sim m_b^2$. No attempts have so far been undertaken to estimate the form factors for intermediate and small q^2 with factorization methods, as done here, which apply when $n_+q \gg \Lambda_{\text{QCD}}$. With these kinematic restrictions the differential branching fraction of the four-lepton decay is expressed, at LP, in terms of generalized inverse moments of the B meson LCDA, which can be related to λ_B .

We consider the case of non-identical lepton flavours, $\ell' \neq \ell$, and identical ones, which requires additional kinematic considerations.

2 Basic definitions

Following the conventions of [5], we write the $B^- \rightarrow \ell \bar{\nu}_\ell \ell' \bar{\ell}'$ decay amplitude to lowest non-vanishing order in the electromagnetic coupling as

$$\begin{aligned}
 A(B^- \rightarrow \ell \bar{\nu}_\ell \ell' \bar{\ell}') &= \frac{G_F V_{ub}}{\sqrt{2}} \langle \ell(p_\ell) \bar{\nu}_\ell(p_\nu) \ell'(q_1) \bar{\ell}'(q_2) | \bar{\ell} \gamma^\mu (1 - \gamma_5) v_\ell \\
 &\quad \cdot \bar{u} \gamma_\mu (1 - \gamma_5) b | B^-(p) \rangle \\
 &= \frac{G_F V_{ub}}{\sqrt{2}} \frac{i e^2}{q^2} Q_\ell [T^{\mu\nu}(p, q) + Q_\ell f_B g^{\mu\nu}] \\
 &\quad \times (\bar{u} \ell' \gamma_\mu v_{\bar{\ell}'})(\bar{u} \ell \gamma_\nu (1 - \gamma_5) v_{\bar{\nu}}), \tag{2.1}
 \end{aligned}$$

where $q \equiv q_1 + q_2$ and $p = m_B v = q + k$, such that $k = p_\ell + p_\nu$ is the momentum of the virtual W boson. In addition, we use the convention $iD^\mu = i\partial^\mu - Q_\ell e A_{\text{em}}^\mu$ for the electromagnetic covariant derivative, with $Q_\ell = -1$ for the lepton fields. The hadronic tensor

$$\begin{aligned}
 T^{\mu\nu}(p, q) &= \int d^4x e^{iq \cdot x} \langle 0 | T \{ j_{\text{em}}^\mu(x), \\
 &\quad (\bar{u} \gamma^\nu (1 - \gamma^5) b)(0) \} | B^- \rangle, \tag{2.2}
 \end{aligned}$$

with the electromagnetic current $j_{\text{em}}^\mu = \sum_q Q_q \bar{q} \gamma^\mu q + Q_\ell \bar{\ell} \gamma^\mu \ell$ accounts for the emission of the virtual photon from the B meson constituents. The second term in the square brackets in (2.1) corresponds to the emission from the final-state lepton, see Fig. 2 below. It can be expressed in terms of the B meson decay constant $\langle 0 | \bar{u} \gamma^\nu (1 - \gamma^5) b | B^-(p) \rangle = -i f_B p^\nu$ and constitutes a power correction relative to the $T^{\mu\nu}$ term in the kinematic region of interest.

The hadronic tensor $T^{\mu\nu}$ can be decomposed into six form factors $F_i(q^2, k^2)$ of two kinematic invariants. Applying the Ward identity $q_\mu T^{\mu\nu} = f_B p^\nu$ leaves four form factors and

a contact term (see Appendix A for details). We write

$$\begin{aligned}
 T^{\mu\nu}(p, q) &= (g^{\mu\nu} v \cdot q - v^\mu q^\nu) \hat{F}_{A_\perp} + i \epsilon^{\mu\nu\alpha\beta} v_\alpha q_\beta F_V \\
 &\quad - \hat{F}_{A_\parallel} v^\mu q^\nu + (q^\mu, k^\nu) \text{ terms.} \tag{2.3}
 \end{aligned}$$

We neglect the lepton masses, in which case the q^μ, k^ν terms drop out after contracting $T^{\mu\nu}(p, q)$ with the lepton tensor. The contact term is fixed by the Ward identity to $(f_B m_B)/(v \cdot q) v^\mu v^\nu$. This can be rewritten as $f_B/(v \cdot q) v^\mu (k^\nu + q^\nu)$ and has been absorbed into \hat{F}_{A_\parallel} and the k^ν terms in (2.3). The convention for the totally anti-symmetric tensor is $\epsilon^{0123} = 1$. The virtual photon emission from the final-state lepton ℓ in (2.1) is exactly cancelled by the redefinition

$$F_{A_\perp} = \hat{F}_{A_\perp} + \frac{Q_\ell f_B}{v \cdot q}, \quad \tilde{F}_{A_\parallel} = \hat{F}_{A_\parallel} - \frac{Q_\ell f_B}{v \cdot q}. \tag{2.4}$$

Therefore, the term in square brackets in (2.1) can be expressed in terms of three form factors. To separate amplitudes corresponding to the different polarization states of the virtual photon, we shall use the decomposition

$$\begin{aligned}
 T^{\mu\nu}(p, q) + Q_\ell f_B g^{\mu\nu} &= F_{A_\perp} g_\perp^{\mu\nu} v \cdot q + i F_V \epsilon^{\mu\nu\alpha\beta} v_\alpha q_\beta \\
 &\quad - F_{A_\parallel} v^\mu q^\nu, \tag{2.5}
 \end{aligned}$$

which implies

$$F_{A_\parallel} = \tilde{F}_{A_\parallel} - \frac{2q^2(m_B^2 - q^2 + k^2)}{\lambda} F_{A_\perp}. \tag{2.6}$$

Here $\lambda \equiv \lambda(m_B^2, q^2, k^2) = m_B^4 - 2m_B^2(k^2 + q^2) + (k^2 - q^2)^2$ the Källén function. The form factor F_{A_\parallel} arises from a longitudinally polarized virtual photon and vanishes in the real-photon limit $q^2 \rightarrow 0$. Without loss of generality we choose the three-momentum \vec{q} to point in the positive z direction, such that its decomposition into light-cone vectors n_\pm^μ reads

$$q^\mu = n_{+q} \frac{n_\pm^\mu}{2} + n_{-q} \frac{n_\mp^\mu}{2}, \tag{2.7}$$

with $n_\pm^\mu = (1, 0, 0, \mp 1)$ and $q^2 = n_{+q} n_{-q}$. The transverse metric tensor is then $g_\perp^{\mu\nu} = g^{\mu\nu} - (n_+^\mu n_-^\nu + n_-^\mu n_+^\nu)/2$. The large component n_{+q} of q^μ is related to the invariant masses q^2 and k^2 via

$$n_{+q} = \frac{m_B^2 - k^2 + q^2 + \sqrt{\lambda}}{2m_B}. \tag{2.8}$$

Finally, we define the left- and right-helicity form factors

$$F_L = \frac{1}{2} (F_V + F_{A_\perp}), \quad F_R = \frac{1}{2} (F_V - F_{A_\perp}). \tag{2.9}$$

Since helicity is conserved in high-energy QCD processes, F_R is power-suppressed relative to F_L in the heavy-quark / large n_+q limit.

For non-identical lepton flavours $\ell \neq \ell'$, the differential decay width can be obtained analytically by a straightforward calculation. The full angular distribution, i.e. the five-fold differential rate is given in Appendix B. Here we quote the double differential rate in the invariant masses q^2 and k^2 , for which we obtain the simple expression

$$\frac{d^2\text{Br}(B^- \rightarrow \ell \bar{\nu}_\ell \ell' \bar{\ell}')}{dq^2 dk^2} = \frac{\tau_B G_F^2 |V_{ub}|^2 \alpha_{\text{em}}^2 \sqrt{\lambda}}{2^8 3^2 \pi^3 m_B^5} \frac{\sqrt{\lambda}}{q^2} \sqrt{1 - \frac{4m_{\ell'}^2}{q^2}} \times \left(1 - \frac{m_\ell^2}{k^2} \right) \left(8k^2 (m_B^2 + q^2 - k^2)^2 |F_{A\perp}|^2 + 8k^2 \lambda |F_V|^2 + \frac{\lambda^2}{q^2} |F_{A\parallel}|^2 \right), \tag{2.10}$$

keeping the lepton masses $m_{\ell^{(\prime)}}$ in the phase space integration (implying $q^2 > 4m_{\ell'}^2$), which is relevant for muons.

The case of identical lepton flavours $\ell' = \ell$ is more complicated, as an additional contribution from the interchange of the two final-state leptons arises. To clarify this point, let us define $B^- \rightarrow \ell^-(p_1)\ell^+(p_2)\ell^-(p_3)\bar{\nu}_\ell(p_\nu)$, with $q^2 = (p_1 + p_2)^2$ and $\tilde{q}^2 = (p_2 + p_3)^2$. At the amplitude level, we have $\mathcal{M}_{\text{tot}} = \mathcal{M}_a - \mathcal{M}_b$ where $\mathcal{M}_b = \mathcal{M}_a(p_1 \rightarrow p_3, p_3 \rightarrow p_1)$. For the decay rate, this results in an additional interference term between \mathcal{M}_a and \mathcal{M}_b , while the rates $\Gamma_{a,b} \propto |\mathcal{M}_{a,b}|^2$ from the squares of the individual diagrams are equal (as depicted in Fig. 1). Since $\Gamma_a + \Gamma_b$ is equal to the rate for non-identical lepton flavours, we find

$$\text{Br}(B^- \rightarrow \ell \bar{\nu}_\ell \ell \bar{\ell}) = \text{Br}(B^- \rightarrow \ell \bar{\nu}_\ell \ell' \bar{\ell}') + \text{Br}_{\text{int}}(B^- \rightarrow \ell \bar{\nu}_\ell \ell \bar{\ell}). \tag{2.11}$$

For the interference term $d^2\text{Br}_{\text{int}}(B^- \rightarrow \ell \bar{\nu}_\ell \ell \bar{\ell})/(dq^2 dk^2)$ can only be obtained numerically.

3 Calculation of the form factors

The amplitude can be factorized through an expansion in Λ_{QCD}/m_b and $\Lambda_{\text{QCD}}/n_+q$, if the quark propagator that connects the electromagnetic and the weak current is far off-shell. This happens for very large q^2 of order m_B^2 in which case the amplitude can be reduced to a hard matching coefficient times the B meson decay constant defined as a local matrix element in heavy-quark effective theory (HQET). The decay rate for such large q^2 is highly suppressed. The situation is more interesting when $q^2 \ll m_B^2$, but q^μ has still a large component $n_+q \sim \mathcal{O}(m_B)$, while $n_-q \sim \mathcal{O}(\Lambda_{\text{QCD}})$, or even smaller. In this case the intermediate quark propagator becomes hard-collinear and the γ^* probes the light-

cone structure of the B meson. A factorization formula, which expresses the form factors as a convolution of the B meson LCDA with a perturbative scattering kernel, can then be derived for the LP contribution using soft-collinear effective theory [13–16] by matching QCD \rightarrow SCET_I \rightarrow HQET. Since the derivation is very similar to the one for $B^- \rightarrow \ell^- \bar{\nu}_\ell \gamma$ and $B_s \rightarrow \mu^+ \mu^- \gamma$ decays [5, 11], we only sketch the main steps in the following.

Upon integrating out the hard scales m_b, n_+q , the flavour-changing weak current is represented in SCET_I by

$$\bar{q} \gamma^\mu (1 - \gamma_5) b \rightarrow C_V^{(A0)} [\bar{q}_{\text{hc}} \gamma_\perp^\mu (1 - \gamma_5) h_\nu] + (C_4 n_-^\mu + C_5 v^\mu) [\bar{q}_{\text{hc}} (1 + \gamma_5) h_\nu], \tag{3.1}$$

with hard matching coefficients $C_i = C_i(n_+q; \mu)$. Here $q_{\text{hc}} = W^\dagger \xi_{\text{hc}}$ is the hard-collinear quark field in SCET, multiplied with a hard-collinear Wilson line to ensure SCET collinear gauge-invariance. Fields without arguments live at space-time point $x = 0$. At LP, the index μ is transverse, since the LP SCET_I electromagnetic current $j_{q,\text{SCET}_I}^\mu(x)$ [3] contains only the transverse polarization of the virtual photon. We therefore only need $C_V^{(A0)}$, which to $\mathcal{O}(\alpha_s)$ reads [13]

$$C_V^{(A0)}(n_+q; \mu) = 1 + \frac{\alpha_s C_F}{4\pi} \left(-2 \ln^2 \frac{m_B z}{\mu} + 5 \ln \frac{m_B z}{\mu} - \frac{3 - 2z}{1 - z} \ln z - 2 \text{Li}_2(1 - z) - \frac{\pi^2}{12} - 6 \right), \tag{3.2}$$

with $\alpha_s \equiv \alpha_s(\mu)$ in the $\overline{\text{MS}}$ scheme, and $z = n_+q/m_B = 1 - k^2/m_B^2 + \mathcal{O}(\Lambda_{\text{QCD}}/m_B)$. The hadronic tensor is then expressed as

$$T^{\mu\nu}(p, q) = 2C_V^{(A0)} T^{\mu\nu}(q) \tag{3.3}$$

in terms of the matching coefficient and the SCET_I correlation function

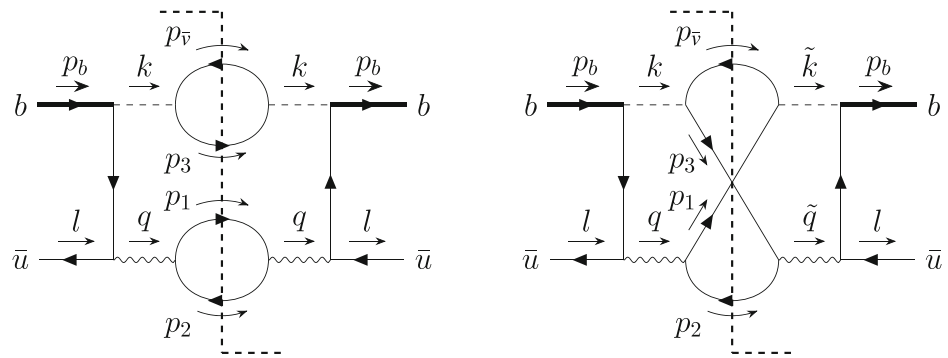
$$T^{\mu\nu}(q) = \int d^4x e^{iqx} \langle 0 | T \left\{ j_{q,\text{SCET}_I}^\mu(x), [\bar{q}_{\text{hc}} \gamma_\perp^\nu P_L h_\nu](0) \right\} | B_v^- \rangle. \tag{3.4}$$

A discussion of the precise power counting of the individual terms in j_{q,SCET_I}^μ and the possibility of extrapolating the above expressions to the large q^2 region with tree-level accuracy can be found in [11].

The SCET_I correlation function is then matched at LP to HQET. This results in

$$T^{\mu\nu}(q) = \left(g_\perp^{\mu\nu} + \frac{i}{2} \epsilon^{\mu\nu\rho\sigma} n_{+\rho} n_{-\sigma} \right) \frac{Q_u F_B m_B}{4} \times \int_0^\infty d\omega \phi_+^B(\omega) \frac{J(n_+q, q^2, \omega; \mu)}{\omega - n_-q - i0^+}, \tag{3.5}$$

Fig. 1 Graphical representation of the squared amplitude for the non-identical-lepton final-state (left) and of the interference term for the case of identical lepton flavours (right)



where $n_{-q} = q^2/n_{+q}$. The hard-collinear matching function [17]

$$J(n_{+q}, q^2, \omega; \mu) = 1 + \frac{\alpha_s C_F}{4\pi} \left\{ \ln^2 \frac{\mu^2}{n_{+q}(\omega - n_{-q})} - \frac{\pi^2}{6} - 1 - \frac{n_{-q}}{\omega} \ln \frac{n_{-q} - \omega}{n_{-q}} \left[\ln \frac{\mu^2}{-q^2} + \ln \frac{\mu^2}{n_{+q}(\omega - n_{-q})} + 3 \right] \right\} \tag{3.6}$$

is convoluted with the leading-twist B meson LCDA $\phi_+^B(\omega)$ defined through

$$\langle 0 | \bar{q}_s(tn_-) [tn_-, 0] \not{v} \gamma_5 h_v(0) | B_v^- \rangle = i m_B F_B \int_0^\infty d\omega e^{-i\omega t} \phi_+^B(\omega), \tag{3.7}$$

which contains the scale-dependent HQET B meson decay constant $F_B = F_B(\mu)$. Similar to the denominator in (3.5), n_{-q} in (3.6) must be understood as $n_{-q} + i0^+$.

As a consequence of helicity conservation of QCD in the high-energy limit, the Lorentz structure in (3.5) gives a non-vanishing contribution only to the left-helicity form factor F_L , which can be expressed as

$$F_L^{\text{LP}} = C_V^{(A0)}(\mu) \frac{Q_u F_B(\mu) m_B}{n_{+q}} \int_0^\infty d\omega \phi_+^B(\omega; \mu) \times \frac{J(n_{+q}, q^2, \omega; \mu)}{\omega - n_{-q} - i0^+}. \tag{3.8}$$

The form factors F_R and $F_{A\parallel}$ vanish at leading power, $F_R^{\text{LP}} = F_{A\parallel}^{\text{LP}} = 0$. The $-i0^+$ prescription in (3.8) generates a rescattering phase of the form factor F_L for $q^2 > 0$.

A factorization formula for NLP corrections is presently not known. Following [5, 11] we infer the leading NLP $\mathcal{O}(\alpha_s^0)$ contributions by a diagrammatic analysis of the tree diagrams of Fig. 2. In the hard-collinear region, diagrams (b) and (c) vanish at LP. Their NLP contribution can be expressed in terms of f_B . In diagram (a), which gives the $\mathcal{O}(\alpha_s^0)$ term in the above LP factorization result, we now expand the light-

quark propagator to NLP, and obtain

$$\frac{(q-l)}{(q-l)^2} = \frac{1}{n_{-q} - \omega} \frac{\not{v}}{2} + \left[\frac{1}{n_{+q}} \frac{\not{v}_+}{2} - \frac{l_\perp}{n_{+q}(n_{-q} - \omega)} + \frac{n_{+l}}{n_{+q}} \frac{\omega}{(n_{-q} - \omega)^2} \frac{\not{v}_-}{2} \right] + \dots, \tag{3.9}$$

where l denotes the spectator-quark momentum of order Λ_{QCD} and terms suppressed by two powers of $\Lambda_{\text{QCD}}/\{n_{+q}, m_b\}$ are neglected. This expression reduces to the one [5] for real photons, when $n_{-q} = 0$ and $n_{+q} = 2E_\gamma$. Proceeding as in [5], we find

$$F_L^{\text{NLP}} = \xi(q^2, v \cdot q) + \frac{Q_\ell f_B}{2v \cdot q}, \tag{3.10}$$

$$F_R^{\text{NLP}} = \frac{F_B m_B Q_u}{n_{+q} n_{+q}} \left(1 + \frac{n_{-q}}{\lambda_B^+(n_{-q})} \right) - \frac{F_B m_B Q_b}{q^2 - 2m_b v \cdot q} - \frac{Q_\ell f_B}{2v \cdot q} \tag{3.11}$$

for the $\mathcal{O}(\alpha_s^0)$ NLP terms of the form factors. These expressions are written in a form such that the complete expression for $F_{L,R}$ including F_L^{LP} is valid for both, hard-collinear and hard q^2 .² Setting $2v \cdot q = n_{+q} + n_{-q} \rightarrow n_{+q}$ and neglecting q^2 in the denominator of the second term in (3.11), one recovers the strict NLP expressions in the hard-collinear region. The q^2 -dependent inverse moment of the B LCDA is defined as

$$\frac{1}{\lambda_B^+(n_{-q})} \equiv \int_0^\infty d\omega \frac{\phi_+^B(\omega)}{\omega - n_{-q} - i0^+}. \tag{3.12}$$

Power corrections to F_L from the photon emission off the spectator quark cannot be factorized and are parametrized by the ‘‘symmetry-preserving’’, power-suppressed form factor

² The absence of a soft form factor in the hard region is respected by our ansatz for $\xi(q^2, v \cdot q)$ below, which makes it a next-to-next-to-leading power correction in the hard region.

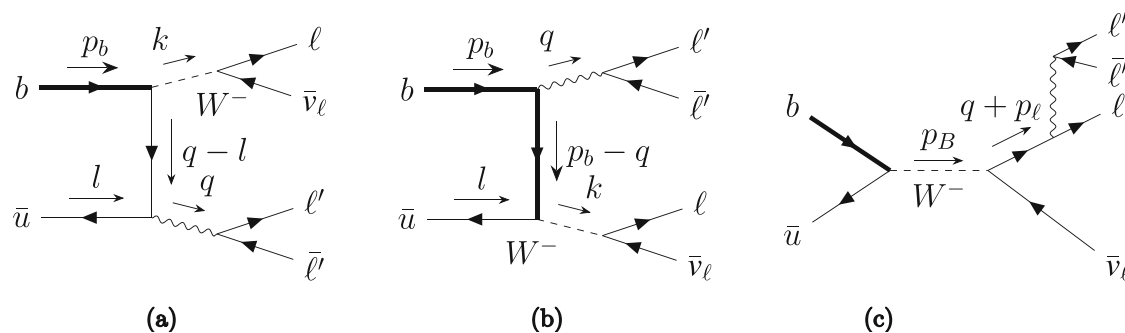


Fig. 2 Photon emissions that contribute to the tree-level $B^- \rightarrow \ell \bar{\nu}_\ell \ell' \bar{\ell}'$ amplitude. The emission from the spectator quark (a) contributes at leading power whereas the emission from the heavy quark (b) and the lepton (c) is power suppressed

$\xi(q^2, v \cdot q)$. For $q^2 \rightarrow 0$ we recover the result for the on-shell $B^- \rightarrow \ell \bar{\nu}_\ell \gamma$ form factors [5].

One important difference between the virtual and on-shell photon case concerns the second term in the square brackets in (3.9), which matches onto a hadronic matrix element with a transverse derivative acting on the spectator-quark field. This term contributes only to the longitudinal form factor $F_{A\parallel}$ and is hence irrelevant in $B \rightarrow \gamma \ell \nu$. Since we do not consider explicitly the tree-level contributions proportional to the three-particle LCDAs of the B meson, we can compute this term in the so-called Wandzura–Wilczek (WW) approximation [18], in which case only the subleading two-particle LCDA $\phi_-^B(\omega)$ appears. We then find, for hard-collinear q^2 ,

$$\begin{aligned}
 F_{A\parallel}^{\text{NLP}} &= -\frac{2F_B Q_u}{n+q} \left(2m_B \frac{n-q}{n+q} \frac{1}{\lambda_B^-(n-q)} + 1 \right) \\
 &\quad + \frac{2F_B(Q_b - Q_\ell)}{n+q} + \xi'(q^2, v \cdot q) \\
 &= -\frac{4F_B m_B Q_u}{(n+q)^2} \frac{n-q}{\lambda_B^-(n-q)} + \xi'(q^2, v \cdot q). \tag{3.13}
 \end{aligned}$$

In the numerical analysis, we employ an expression for $F_{A\parallel}$, which is accurate in both the hard and hard-collinear q^2 region. To this end, we use (2.6) together with

$$\begin{aligned}
 \tilde{F}_{A\parallel}^{\text{NLP}} &= \frac{4F_B m_B Q_u}{n+q} \frac{n-q}{n+q} \left(\frac{1}{\lambda_B^+(n-q)} - \frac{1}{\lambda_B^-(n-q)} \right) \\
 &\quad - \frac{2F_B Q_u}{n+q} \left(1 + \frac{n-q}{\lambda_B^+(n-q)} \right) \\
 &\quad + \frac{2F_B m_b Q_b}{2v \cdot q m_b - q^2} - \frac{2f_B Q_\ell}{2v \cdot q} + \xi'(q^2, v \cdot q), \tag{3.14}
 \end{aligned}$$

and $F_{A\perp}^{\text{NLP}}$ computed from (3.10), (3.11). The inverse moment $\lambda_B^-(n-q)$ of the subleading-twist LCDA $\phi_-^B(\omega)$, which was already introduced for $B \rightarrow K^* \ell \ell$ [19], is defined in anal-

ogy to (3.12). The finite invariant mass of the virtual photon regulates its endpoint divergence at $\omega \rightarrow 0$. Nevertheless, in the limit $q^2 \rightarrow 0$ we find $F_{A\parallel} \rightarrow 0$ due to the additional $n-q$ in the numerator, as it should be, since an on-shell photon has no longitudinal polarization. As in the case of F_L we allow for a possible non-factorizable contribution by adding an unknown form factor $\xi'(q^2, v \cdot q)$, which must also vanish as $q^2 \rightarrow 0$.

The power-suppressed form factor ξ that parameterizes the contribution from soft distances $x \sim 1/\Lambda_{\text{QCD}}$ between the currents in $T^{\mu\nu}$ as well as the three-particle B LCDA contributions have been calculated with light-cone QCD sum rules [17,20], but this method can only be used for $q^2 = 0$ or space-like. We therefore follow the simple ansatz [11]

$$\begin{aligned}
 \xi(q^2, v \cdot q) &= -r_{\text{LP}} \frac{F_B m_B Q_u}{n+q} \frac{1}{\lambda_B^+(n-q)} \\
 \xi'(q^2, v \cdot q) &= 0, \tag{3.15}
 \end{aligned}$$

which incorporates the observation that the power-suppressed form factors appear to reduce the LP ones by setting them to a fraction $r_{\text{LP}} = 0.2$ of F_L at tree level. Since there is no LP contribution to $F_{A\parallel}$, ξ' is set to 0 in this model. The branching fraction of the four-lepton decay is quite sensitive to the value of r_{LP} . For the $B_s \rightarrow \mu^+ \mu^- \gamma$ decay the conservative estimate $r_{\text{LP}} = 0.2 \pm 0.2$ was adopted [11]. Below we also present results for $r_{\text{LP}} = 0.2 \pm 0.1$.

Since the $B \rightarrow \gamma^*$ form factors are time-like, the heavy-quark/large-energy expansion is certainly upset locally by the lowest light-meson resonances, ρ and ω . However, as shown in [11], quark–hadron duality is also violated globally, such that for any q^2 bin that contains these resonances, the resonance contribution will be dominant. In order to describe the form factors in the entire region $q^2 \lesssim 6 \text{ GeV}^2$, we add the resonant process $B^- \rightarrow \ell \bar{\nu}_\ell V \rightarrow \ell \bar{\nu}_\ell \ell^{(\prime)} \bar{\ell}^{(\prime)}$, where $V = \rho, \omega$, to the factorization expressions (3.10) and (3.11). As discussed in [11], this procedure can be justified parametrically, as the averaged resonance contribution is formally a

power correction. Nevertheless, the existence of resonances implies that the QCD factorization calculation of the time-like form factors is not on as solid ground as at $q^2 = 0$ for $B^- \rightarrow \ell^- \bar{\nu}_\ell \gamma$. Writing the dispersion relation in q^2 at fixed $n+q$ for the hadronic tensor $T^{\mu\nu}$, and including only the ρ and ω resonances in the spectral function in the Breit–Wigner approximation, we find

$$F_{L(R)}^{\text{res}} = \sum_{V=\rho^0, \omega} \text{BW}_V \frac{1}{2} \left(\frac{2m_B}{m_B + m_V} V^{B \rightarrow V}(k^2) \pm \frac{m_B + m_V}{v \cdot q} A_1^{B \rightarrow V}(k^2) \right), \tag{3.16}$$

where the upper (lower) sign applies to F_L (F_R). In addition,

$$\text{BW}_V \equiv c_V \frac{f_V m_V}{m_V^2 - q^2 - i m_V \Gamma_V}, \tag{3.17}$$

with $c_\rho = 1/2$ and $c_\omega = 1/6$.³ For the $B \rightarrow V$ transition form factors V, A_1 and A_2 we use the definition and numerical results of [21]. It follows from the heavy-quark symmetry relations for the heavy-to-light $B \rightarrow V$ form factors [18], (applicable since $k^2 = k^2(n+q, q^2)$ via (2.8) and $n+q \gg \Lambda_{\text{QCD}}$ and $q^2 = m_V^2$ in the argument of the form factors in (3.16)) that F_R^{res} is power-suppressed relative to F_L^{res} , hence it formally counts as a next-to-next-to-leading power correction. We do not add a resonance contribution to the form factor F_{A_\parallel} for the longitudinal intermediate polarization state, since a simple Breit–Wigner ansatz as above would lead to a non-vanishing form factor at $q^2 = 0$ resulting in a $1/q^4$ singularity in the rate, which is unphysical.⁴

4 Numerical results

We combine the form factors at leading-power (LP) and next-to-leading power (NLP) calculated with QCD factorization with the resonance contribution into the final result

$$F_X = F_X^{\text{LP}} + F_X^{\text{NLP}} + F_X^{\text{res}}. \tag{4.1}$$

We include renormalization group evolution to sum logarithms of the ratio of the hard, hard-collinear and soft scales in the LP term following [5], but not in F_X^{NLP} where we set

³ Compared to [11], c_ρ has opposite sign because it arises from the $u\bar{u}$ content of the ρ meson, while in [11] the $d\bar{d}$ component was the relevant one.

⁴ We note that such an ansatz has been used in [9,10]. We remark that $F_{L(R)}^{\text{res}}$ retains an unphysical imaginary part at $q^2 = 0$ from (3.17), which, however, is even further suppressed by the small width $\Gamma_V/m_V \ll 1$ of the resonances.

Table 1 Input parameters from PDG [24] unless stated otherwise. The value of f_B is taken from FLAG [23] using inputs from [25–28]. Here we quote the exclusive $|V_{ub}|$ value from HFLAV [22], which uses lattice inputs from [29,30]. Here $\alpha_{\text{em}} = \alpha_{\text{em}}^{(5)}(5 \text{ GeV})$

Parameter	Value	Parameter	Value
$ V_{ub} $	$3.70 \cdot 10^{-3}$ [22]	α_{em}	1/132.18
m_b	4.78 GeV	f_B	190 MeV [23]
m_ρ	770 MeV	m_ω	782 MeV
Γ_ρ	147.8 MeV	Γ_ω	8.49 MeV
f_ρ	213 MeV [21]	f_ω	197 MeV [21]

$F_B = f_B$. Contrary to [11], we do not re-expand products of series expansions in α_s .

We use the inputs specified in Table 1 and the exponential model

$$\phi_+^B(\omega) = \frac{\omega}{\omega_0^2} e^{-\omega/\omega_0}, \quad \phi_-^B(\omega) = \frac{1}{\omega_0} e^{-\omega/\omega_0}, \tag{4.2}$$

for the B LCDA. We put $\omega_0 = \lambda_B \equiv \lambda_B^+(n-q=0) = 0.35 \pm 0.15 \text{ GeV}$ at the scale 1 GeV as our default value. In the LP terms, we evolve $\phi_+^B(\omega)$ to the hard-collinear scale μ_{hc} employing the analytic expression given in [20]. Previous analyses of $B \rightarrow \gamma \ell \nu$ showed that the shape of the B LCDA is also important when including power corrections [20]. For the time-like virtual photon form factors, there is less control over power corrections and we therefore content ourselves with the exponential model to present our main results and conclusions. We further study the dependence of $\lambda_B^\pm(n-q)$ and the branching fraction of the four-lepton decay on the shape of the B meson LCDA in Sec. 4.4 using three two-parameter models [20] for the B LCDA. In addition, as $|V_{ub}|$ is an overall factor we do not include its uncertainty in our error estimates, nor do we include the negligible uncertainties on the other input parameters in Table 1. We expect that eventual measurements of the four-lepton final states will be normalized to the decay rate of another, accurately known, exclusive $b \rightarrow u$ transition.

4.1 Form factors

In Fig. 3, we show $|F_L^{\text{LP}}|$ at leading order (LP,LO) and next-to-leading order (LP,NLO) as a function of q^2 at fixed $n+q = 4 \text{ GeV}$. The band describes the scale uncertainty of the hard-collinear scale $\mu_{hc} = 1.5 \pm 0.5 \text{ GeV}$ (left) and that of the hard scale $\mu_h = 5_{-2.5}^{+5} \text{ GeV}$ (right). Similar to the $B \rightarrow \gamma \ell \nu$ case, at small q^2 the form factor in the LO approximation has a large scale uncertainty, which is practically removed by the NLO correction. We conclude that the LP form factor is under very good control away from light-meson resonances, once the B LCDA input is specified. It is worth noting that the

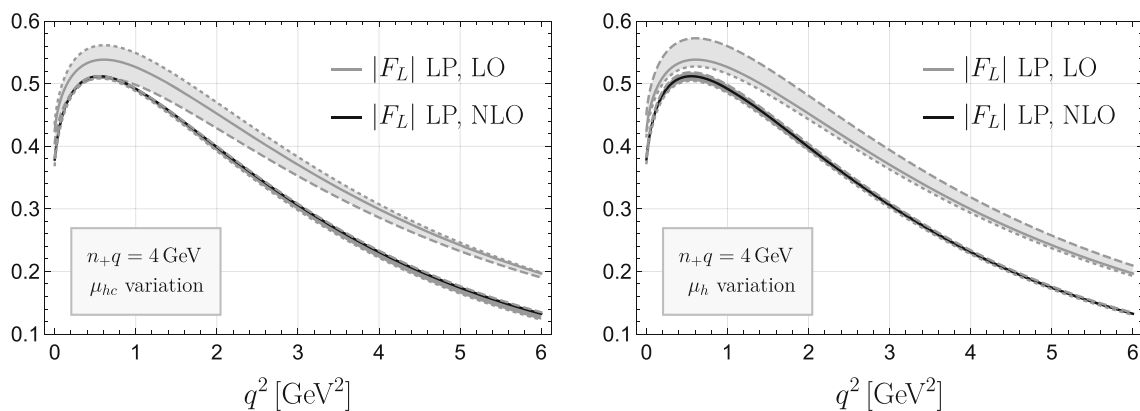


Fig. 3 $|F_L^{\text{LP}}|$ at leading order (LP, LO) and next-to-leading order (LP, NLO) as a function of q^2 . The bands represent the scale uncertainty from $\mu_{hc} = 1.5 \pm 0.5$ GeV (left) and $\mu_h = 5^{+5}_{-2.5}$ GeV (right) and the

dashed (dotted) curves correspond to the upper (lower) scale value. The value of n_+q is fixed to 4 GeV

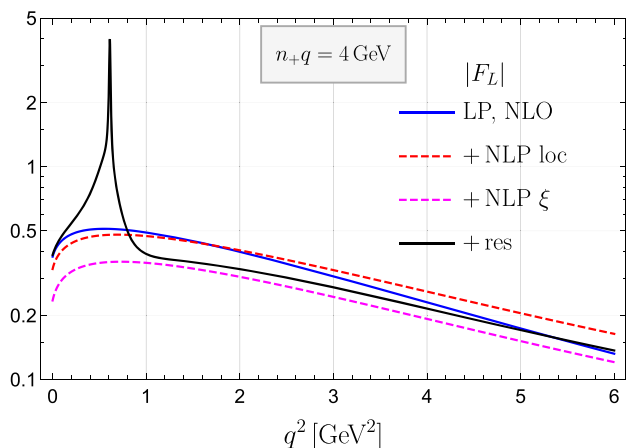


Fig. 4 Illustration of the q^2 dependence of the leading form factor $|F_L|$ including successively leading power (LP, NLO), next-to-leading power (NLP) local contributions, ξ and resonances. The value of n_+q is fixed to 4 GeV

form factors do not fall off right away with increasing q^2 , but exhibit a maximum near $q^2 \approx 0.5$ GeV². The maximum is generated by the sizeable imaginary part $\pi\phi_+^B(n-q)$ of the q^2 -dependent B LCDA moment $\lambda_B^+(n-q)$. These features of F_L are largely independent of the chosen value of n_+q .

The breakdown of $|F_L|$ into its various contributions is shown in Fig. 4, starting with LP,NLO, then successively adding the NLP local (loc) contributions (defined as F_X^{NLP} without the ξ term), the ξ -contribution as defined in (3.15) and finally the resonance contribution (res). We observe that the NLP contribution is of similar size as the NLO correction at LP. In the small q^2 region, the form factor is locally dominated by the resonance contribution, as expected. However, also at larger q^2 the resonance contribution is comparable to the NLP local contribution. This is due to the fact that the

fall-off of the form factors in QCD factorization with increasing q^2 is not faster than the $1/q^2$ fall-off of the Breit–Wigner parametrization of the resonances. Note that we have fixed again $n_+q = 4$ GeV, and only show the q^2 dependence of the form factors as the above observations are generic.

The q^2 dependence of the power-suppressed (NLP) form factors F_R and $F_{A\parallel}$ is shown in the lower panel of Fig. 5. For F_R , we show separately the local NLP contribution and the total by adding the resonance contribution. As we do not include a resonance contribution for $F_{A\parallel}$, we only show the total form factor. In addition, we show the dependence on λ_B by varying it from 200 MeV (dashed) to 500 MeV (dotted). Except for very small q^2 , the form factor relevant to the longitudinal polarization state of the virtual photon is significantly larger than the one for the right-helicity state.

For F_L (upper panel of Fig. 5), we show in addition to the results for $\lambda_B = 200$ MeV (dashed) and 500 MeV (dotted) the dominant uncertainty of $|F_L|$ computed with the central value $\lambda_B = 350$ MeV from varying r_{LP} by $\delta r_{\text{LP}} = 0.1(0.2)$. We note two important features. First, for all three form factors there is a crossing of the dashed and dotted lines, such that the lower value $\lambda_B = 200$ MeV increases the form factors at small q^2 but decreases it for large q^2 , while for the upper value $\lambda_B = 500$ MeV the situation is reversed. In the region where the crossing occurs (around 3.5 GeV² for F_L) all sensitivity to λ_B is lost. Second, for F_L at low q^2 the sensitivity to λ_B is larger than the uncertainty coming from r_{LP} .

Finally, we comment on the contribution of the three form factors to the differential rate in (2.10). More precisely, we show in Fig. 6 the three terms in the round bracket in (2.10), that is, the form factors squared including their kinematic prefactors. It is remarkable that the longitudinal polarization term $\frac{\lambda^2}{q^2} |F_{A\parallel}|^2$ dominates the rate outside the reso-

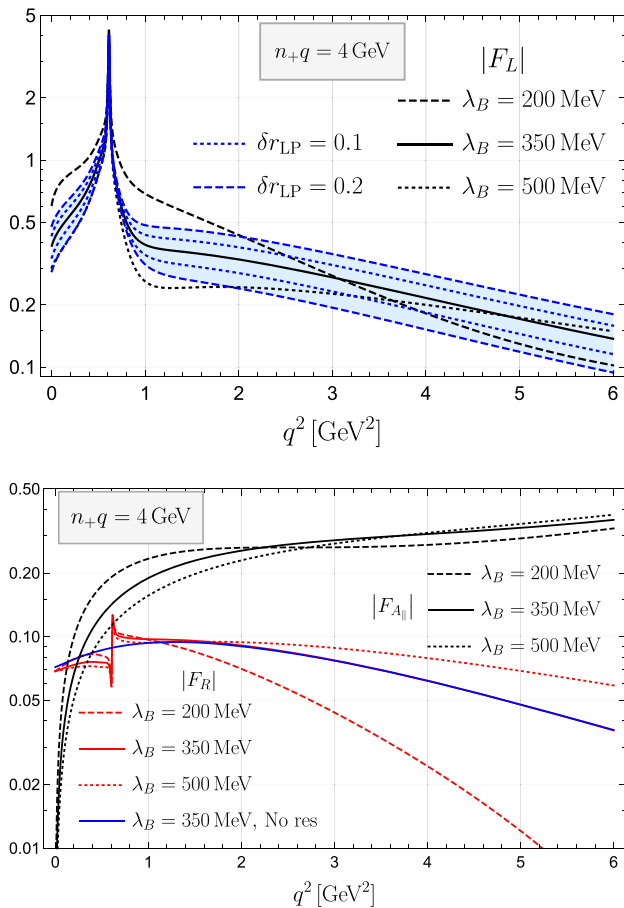


Fig. 5 The q^2 dependence of the form factors at fixed $n_+q = 4$ GeV for three values of λ_B from 200 MeV (dashed) to 500 MeV (dotted). In addition, for $|F_L|$ (upper panel) we show the uncertainty from varying for the central value r_{LP} by $\delta r_{LP} = 0.1(0.2)$. For the NLP form factors (lower panel), we show $|F_R|$ for both, with and without the resonance contribution. We do not add a resonance contribution to $F_{A\parallel}$

nance region, despite that fact that it is technically power-suppressed. Moreover, leaving out the resonance term, the longitudinal term would dominate even at small q^2 , although it vanishes for $q^2 \rightarrow 0$ (since $F_{A\parallel} \sim q^2$ as $q^2 \rightarrow 0$), while the other two terms approach constants in this limit.

This behaviour can be understood by comparing the analytic expressions for the three terms (without the resonance term) for small q^2 . For small q^2 , the first two terms in the round bracket of (2.10) combine to $16k^2(m_B^2 - k^2)^2(|F_L|^2 + |F_R|^2)$, and we then estimate

$$\begin{aligned} \frac{d^2\text{Br}^{(F_{A\parallel})}}{dq^2 dk^2} / \frac{d^2\text{Br}^{(F_L)}}{dq^2 dk^2} &= \frac{m_B}{m_B - n_+q} \frac{q^2}{(n_+q)^2} \left(\ln^2 \frac{q^2 e^{\gamma_E}}{n_+q \lambda_B^+} + \pi^2 \right) \\ &\quad + \mathcal{O}\left(\frac{q^4}{m_B^4}\right) \\ &\approx \frac{27\pi^2 q^2}{4m_B^2} + \mathcal{O}\left(\frac{q^4}{m_B^4}\right), \end{aligned} \tag{4.3}$$

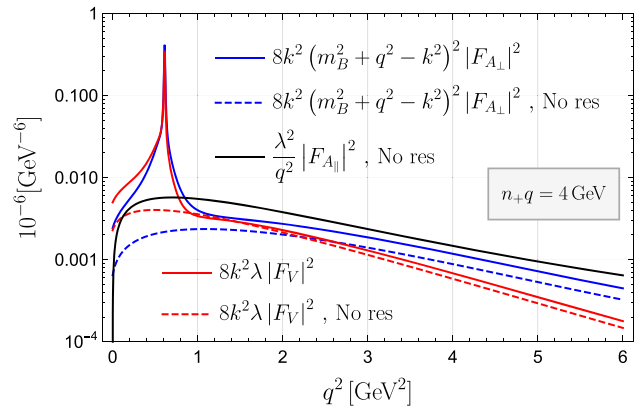


Fig. 6 Contribution of the form factors to the rate in (2.10) including kinematic factors. For F_V and $F_{A\perp}$, we show the QCDF results (labelled “No res”) and the full result including resonances

where the last line refers to the representative value $n_+q = 2m_B/3$. The parametric dependence identifies this ratio as power-suppressed in the hard-collinear region $q^2 \sim m_B \Lambda_{\text{QCD}}$ as it should be. However, the large numerical factor $27\pi^2/4$ implies that the longitudinal term dominates whenever q^2 is larger than the very small value 0.4 GeV^2 as seen in the Figure. The origin of the large factor is the π^2 that arises from the large imaginary part of the inverse B LCDA moment, in this case $\lambda_B^-(n-q)$ in (3.13), since for values $q^2 \in [0.1, 1] \text{ GeV}^2$ the logarithmic term $\ln^2 \frac{q^2 e^{\gamma_E}}{n_+q \lambda_B^+}$ is small.

4.2 Predictions for the branching ratios

In this section, we provide theoretical predictions for the branching ratio in various q^2 bins, integrated over n_+q (alternatively, k^2). The factorization calculation of the form factors in (3.8), (3.10), (3.11) and (3.13) are valid only for $n_+q \sim \mathcal{O}(m_B)$. We therefore assume $n_+q > 3 \text{ GeV}$, which corresponds to $E_\gamma = 1.5 \text{ GeV}$ at $q^2 = 0$, and integrate the double-differential branching fraction over $n_+q > 3 \text{ GeV}$ before forming q^2 bins. A rough estimate, obtained by assuming that our results apply in the full phase space, shows that the n_+q cut reduces the rate by $\mathcal{O}(20\%)$ for the $[1.5, 6] \text{ GeV}^2$ q^2 bin.

For non-identical lepton flavours, $\ell' \neq \ell$, the required n_+q cut can easily be applied as for each event n_+q can be inferred from the reconstructed k^2 and q^2 using (2.8). For the q^2 bins, we consider the low bin $[4m_\mu^2, 0.96] \text{ GeV}^2$, where the upper boundary of the bin is determined such that the large experimental background from ϕ mesons decaying into a lepton pair is avoided. This bin was also considered by the LHCb Collaboration [8]. Figure 5 shows that in this bin, the ρ and ω resonances make a large contribution. As mentioned, we do not attribute an additional error due to our resonance model. This introduces an additional uncertainty in this region which

Table 2 Branching ratio for the two non-identical lepton flavour cases (in 10^{-8}) integrated over different bins in q^2 and for $n+q > 3$ GeV. We show the individual contributions consecutively adding to the LP result the NLP local and ξ contributions and finally the resonances.

Decay	q^2 bin (GeV ²)	LP		NLP		Total	Uncertainty			
		LO	NLO	loc	+ ξ		+res	$\mu_{h,hc}$	r_{LP}	λ_B
$\mu^- \mu^+ e^- \bar{\nu}_e$	$[4m_\mu^2, 0.96]$	0.58	0.51	0.70	0.48	1.57	+0.02	+0.35	+1.33	+1.37
	$[4m_\mu^2, 6]$	0.76	0.66	0.98	0.67	1.78	-0.02	-0.29	-0.40	-0.49
	[1, 6]	0.18	0.14	0.26	0.18	0.20	+0.02	+0.43	+1.46	+1.52
	[1.5, 6]	0.10	0.08	0.15	0.10	0.11	-0.02	-0.35	-0.47	-0.58
	[2, 6]	0.062	0.042	0.090	0.062	0.068	+0.00	+0.08	+0.11	+0.14
$e^- e^+ \mu^- \bar{\nu}_\mu$	$[q_{\min}^2, 0.96]$	1.23	1.04	1.23	0.81	2.28	-0.00	-0.06	-0.06	-0.08
	[1, 6]	0.18	0.14	0.26	0.18	0.20	+0.00	+0.08	+0.11	+0.14
							-0.00	-0.06	-0.06	-0.08

In addition, we quote the uncertainties from varying the scales $\mu_{h,hc}$, $r_{LP} = 0.2 \pm 0.2$ and $\lambda_B = 350 \pm 150$ MeV. The total uncertainty is obtained by adding them in quadrature. For electrons, we also consider a low bin with $q_{\min}^2 = 0.0025$ GeV²

is challenging to quantify. Above $q^2 > 1$ GeV², the effect of the ρ and ω resonances (and thus a possible uncertainty associated with this) is significantly reduced. We consider three different q^2 bins: [1, 6], [1.5, 6] and [2, 6] GeV². In these bins, the resonance contribution is approximately 10% only. In Table 2, we give the branching ratio in these q^2 bins, specifying the contributions which are successively added. In addition, we specify the uncertainties from variations of the scales $\mu_{h,hc}$, $r_{LP} = 0.2 \pm 0.2$ and $\lambda_B = 350 \pm 150$ MeV. We observe that in the three considered regions above $q^2 > 1$ GeV², the effect of the resonances is smaller than the uncertainty from r_{LP} .

4.2.1 Identical lepton flavours

A challenge arises when considering identical lepton flavours, $\ell' = \ell$, because experimentally the two like-sign leptons cannot be distinguished. This results in the additional interference term (2.11). More challenging is the required cut on $n+q$, where q is the photon momentum, to ensure that the photon has hard-collinear momentum. Considering again $B^- \rightarrow \ell^-(p_1)\ell^+(p_2)\ell^-(p_3)\bar{\nu}_\ell(p_\nu)$, with $q^2 = (p_1 + p_2)^2$ and $\tilde{q}^2 = (p_2 + p_3)^2$, experimentally, q^2 and \tilde{q}^2 cannot be distinguished. Instead, the invariant mass of two $\mu^- \mu^+$ -pairs are defined as $q_{\text{low}}^2 < q_{\text{high}}^2$. In this case, placing the required cut on $n+q$ is not unambiguously possible as we cannot determine if the virtual photon has q_{low}^2 or q_{high}^2 associated with its momentum. To deal with this issue, several observations can be made:

- for small q_{low}^2 , the photon momentum can be associated with q_{low}^2 most of the time. If this is the case, a cut on $n+q_{\text{low}} > 3$ GeV suffices (similar to the non-identical lepton flavour case). In fact, a more detailed analysis shows that the cases falling outside this cut (i.e. the region which cannot be described in QCD factorization in which

the photon has q_{high}^2 but $n+q$ small) is phase-space suppressed by two powers of $1/m_b$ compared to the leading contribution.

- for q^2 bins above 1 GeV², the situation is more complicated as the photon more often has q_{high}^2 . Therefore, we have to ensure $n+q > 3$ GeV for both q_{low}^2 and q_{high}^2 .

We thus have to restrict both $n+q_{\text{low}} > 3$ GeV and $n+q_{\text{high}} > 3$ GeV. These quantities are now defined in the following way⁵: for each event, we specify q_{low}^2 and q_{high}^2 . We can then associate the remaining lepton plus neutrino as k_{low}^2 and k_{high}^2 , respectively. Here high and low are just labels and in this case k_{low}^2 is not necessarily lower than k_{high}^2 . Then using (2.8), both $n+q_{\text{low}}$ and $n+q_{\text{high}}$ can be calculated from their corresponding k^2 and q^2 . Alternatively, one could cut on k_{low}^2 and k_{high}^2 directly.

For our final results in Table 3, we thus include two cuts: $n+q_{\text{low}} > 3$ GeV and $n+q_{\text{high}} > 3$ GeV for all bins. Our final results for the branching ratio for different q_{low}^2 bins are given in Table 3. Again we present the different contributions added successively. We emphasize that placing these two cuts on $n+q$ might be conservative, specifically for the low q^2 bin as discussed above, given the phase space suppression of the region in which q_{high}^2 is associated with the photon. We confirm numerically that indeed this region is small, by calculating the rate with and without the cut on $n+q_{\text{high}}$. For comparison, in Table 3 we also give the results for the total rate with only the $n+q_{\text{low}}$ cut in parenthesis. For identical lepton flavours, the branching ratio contains two contributions as defined in (2.11). With this convention, we find that

⁵ We remark that, unlike previously, here $n+q_{\text{high}}$ does not coincide with the component of q_{high}^μ in the n_μ^μ direction as defined above (2.8), Footnote 5 continued if the momentum of the γ^* is q_{low}^μ . The reason is that we always align the z -axis with the three-momentum of the γ^* , but we do not know which of q_{low}^μ and q_{high}^μ refers to the virtual photon momentum.

Table 3 Branching ratio for the two identical lepton cases (in 10^{-8}) integrated over different bins in q_{low}^2 applying two cuts: $n_+q_{\text{low}} > 3$ GeV and $n_+q_{\text{high}} > 3$ GeV. We show the individual contributions consecutively adding to the LP result the NLP local and ξ contributions and finally the resonances. In addition, we quote the uncertainties from

varying the scales $\mu_{h,hc}$, $r_{\text{LP}} = 0.2 \pm 0.2$ and $\lambda_B = 350 \pm 150$ MeV. The total uncertainty is obtained by adding these contribution in quadrature. For the total results, we also quote the result with only one cut: $n_+q_{\text{low}} > 3$ GeV in parenthesis. For electrons, we also consider a low bin with $q_{\text{min}}^2 = 0.0025$ GeV 2

Decay	q_{low}^2 bin (GeV 2)	LP		NLP		Total	Uncertainty			
		LO	NLO	loc	$+\xi$		$+\text{res}$	$\mu_{h,hc}$	r_{LP}	λ_B
$\mu^- \mu^+ \mu^- \bar{\nu}_\mu$	$[4m_\mu^2, 0.96]$	0.58	0.51	0.71	0.49	1.54 (1.77)	+0.02 -0.02	+0.35 -0.29	+1.29 -0.39	+1.34 -0.48
	$[4m_\mu^2, 6]$	0.74	0.64	0.97	0.67	1.75 (2.00)	+0.02 -0.02	+0.42 -0.34	+1.40 -0.45	+1.46 -0.56
	[1, 6]	0.15	0.11	0.25	0.17	0.19 (0.21)	+0.00 -0.00	+0.07 -0.05	+0.10 -0.05	+0.12 -0.06
	[1.5, 6]	0.08	0.06	0.14	0.10	0.11 (0.11)	+0.01 -0.01	+0.04 -0.03	+0.03 -0.02	+0.05 -0.04
	[2, 6]	0.04	0.03	0.08	0.06	0.06 (0.07)	+0.00 -0.00	-0.02 -0.02	+0.00 -0.01	+0.03 -0.02
$e^- e^+ e^- \bar{\nu}_e$	$[q_{\text{min}}^2, 0.96]$	1.22	1.03	1.23	0.80	2.23 (2.57)	+0.04 -0.06	+0.65 -0.53	+2.33 -0.65	+2.42 -0.82
	[1, 6]	0.15	0.12	0.25	0.18	0.20 (0.22)	+0.00 -0.00	+0.07 -0.05	+0.10 -0.05	+0.12 -0.07

Br_{int} contributes positively to the rate but is suppressed by at least one order of magnitude compared to the non-identical lepton flavour rate.

A comment on the low- q^2 bin for $B^- \rightarrow \mu^- \mu^+ \mu^- \bar{\nu}_\mu$ is in order. Our prediction for $\text{Br}(B^+ \rightarrow \mu^- \mu^+ \mu^- \bar{\nu}_\mu)$ is $1.54 (1.77) \cdot 10^{-8}$ and includes cuts on n_+q . Yet, it lies close to the upper limit $< 1.6 \cdot 10^{-8}$ given by the LHCb collaboration for this decay mode in this bin [8]. Hence the LHCb result may already point towards a larger value of λ_B .

4.3 Sensitivity to λ_B

Our predictions for the branching ratio suffer from a large uncertainty due to λ_B . Therefore, a measurement of the branching ratio may be used to obtain a bound on λ_B . Figure 7 shows the rate as a function of λ_B for the $[4m_\mu^2, 0.96]$ GeV 2 bin and for the [1, 3] and [3, 6] GeV 2 bins. We have split the [1, 6] GeV 2 to avoid integrating over the region where the sensitivity to λ_B variation switches sign (see Fig. 5). As the uncertainty of the branching ratio is dominated by the error on r_{LP} , we consider two options; $\delta r_{\text{LP}} = 0.2$ and $\delta r_{\text{LP}} = 0.1$. The latter option shrinks the error by half. These predictions include our model for the long-distance resonance contributions as described above, for which we do not add an uncertainty. We note that the sensitivity to λ_B is best for the small q^2 bins, while it is significantly reduced for higher q^2 bins. Comparing to $B \rightarrow \gamma \ell \nu_\ell$ [20], we conclude that the sensitivity to λ_B for $B \rightarrow \ell \nu_\ell \ell' \bar{\ell}'$ in the low- q^2 bin is comparable (compare to Fig. 5 in [5]) for $\lambda_B < 200$ MeV, but less when it is larger. However, in this bin the resonance contribution is sizeable and there is unquantified model dependence related to its interference with the factorization contribution. For the [1, 3] GeV 2 bin, the resonance contribution is less pronounced and thus this bin could still provide information on λ_B despite its smaller sensitivity.

4.4 Dependence on the shape of the B LCDA

Up to now, we used the exponential model (4.2) to present our main results. However, it is known that for $B \rightarrow \gamma \ell \nu$ [20] the shape of the B meson LCDA has a significant effect through the dependence of radiative corrections on the logarithmic inverse moments, and of the power-suppressed form factor ξ through its dependence on the shape of the LCDA in the sum rule calculation. In four-lepton decay the generalized inverse moments $\lambda_B^\pm(n-q)$ introduce further dependence on the shape of the LCDA.

To study this dependence, we consider three two-parameter models [20]

$$\begin{aligned} \phi_+^{\text{I}}(\omega) &= \left[(1-a) + \frac{a\omega}{2\omega_0} \right] \frac{\omega}{\omega_0^2} e^{-\omega/\omega_0} \quad 0 \leq a \leq 1 \\ \phi_+^{\text{II}}(\omega) &= \frac{1}{\Gamma(2+a)} \frac{\omega^{1+a}}{\omega_0^{2+a}} e^{-\omega/\omega_0} \quad -0.5 < a < 1 \\ \phi_+^{\text{III}}(\omega) &= \frac{\sqrt{\pi}}{2\Gamma(3/2+a)} \frac{\omega}{\omega_0^2} e^{-\omega/\omega_0} U(-a, 3/2-a, \omega/\omega_0) \\ & \quad 0 < a < 0.5, \end{aligned} \quad (4.4)$$

where $U(\alpha, \beta, z)$ is the confluent hypergeometric function of the second kind. Given (ω_0, a) one determines λ_B and the dimensionless shape parameter $\hat{\sigma}_1$, related to the first inverse-logarithmic moment. The range of a is chosen such that the range $-0.693147 < \hat{\sigma}_1 < 0.693147$ is covered, where $\hat{\sigma}_1 = 0$ in the exponential model, see [20] for more details. To study the influence of the shape of the LCDA, we are then interested in the envelope of theoretical predictions of all three models spanned by the variation of a for given λ_B . For simplicity, we assume that these forms of the B meson LCDA hold at the scale $\mu_{hc} = 1.5$ GeV, so that no renormalization group evolution to the hard-collinear scale needs to be performed. We obtain $\phi_-(\omega)$ using the Wandzura–Wilczek

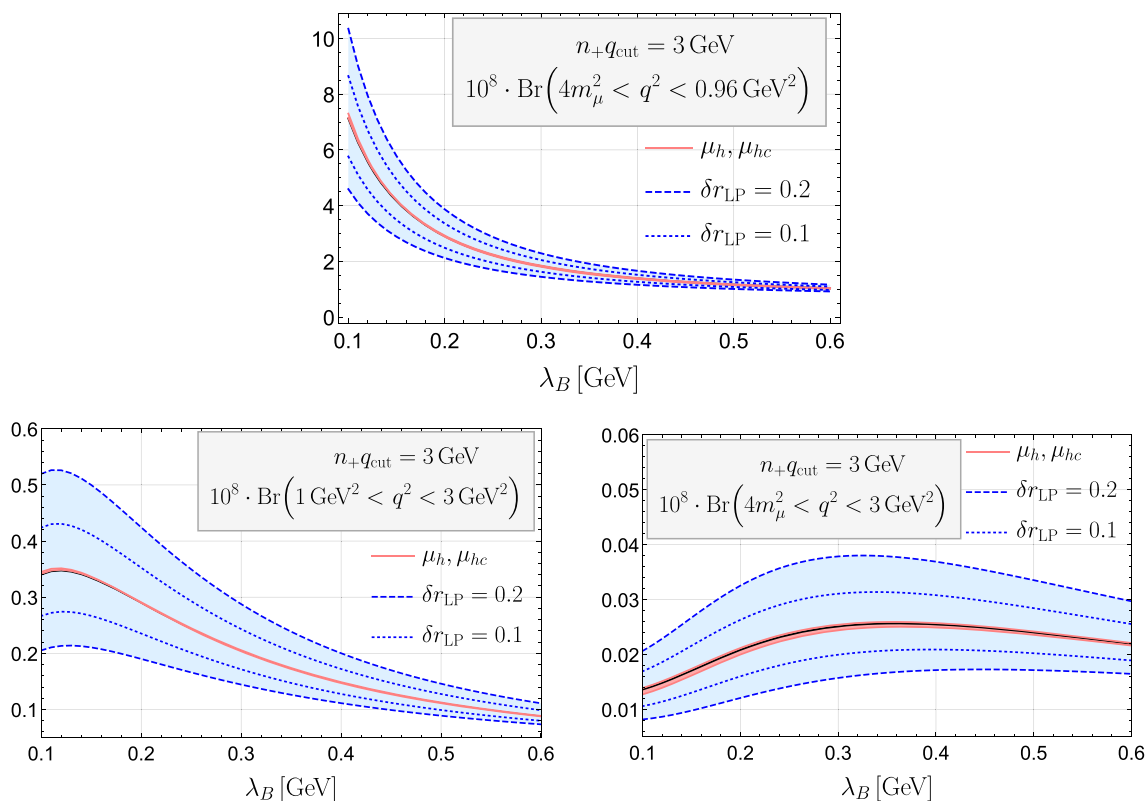


Fig. 7 Branching ratio (in 10^{-8}) for three different q^2 bins as a function of λ_B for the decay mode $B^- \rightarrow \mu^- \mu^+ e^- \bar{\nu}_e$. We include the variation from $\mu_{h,hc}$ and from δr_{LP} as inner (red) and outer (blue) bands, respectively

(WW) relation [18]

$$\phi_-(\omega) = \int_{\omega}^{\infty} \frac{d\omega'}{\omega'} \phi_+(\omega'). \tag{4.5}$$

The $n-q$ dependent moments $\lambda_B^{\pm}(n-q)$ are then obtained using (3.12) (and equivalently for $\lambda_B^-(n-q)$). Again we define $\lambda_B \equiv \lambda_B^+(n-q = 0)$, such that ω_0 can be related to λ_B via

$$\begin{aligned} \omega_0^I &= \lambda_B \left(1 - \frac{a}{2}\right), \\ \omega_0^{II} &= \frac{\lambda_B}{1+a}, \\ \omega_0^{III} &= \frac{\lambda_B}{1+2a}. \end{aligned} \tag{4.6}$$

In Figs. 8 and 9, respectively, we show the q^2 dependence of $1/\lambda_B^+(n-q)$ and $1/\lambda_B^-(n-q)$ for fixed $n+q = 4$ GeV for the three B LCDA models by varying the parameter a within the ranges indicated in (4.4), fixing $\lambda_B = 350$ MeV. The black solid line represents the exponential model. There is a significant dependence of $1/\lambda_B^+(n-q)$ on the B -meson LCDA shape – this is expected, as for instance, the q^2 dependence of the imaginary part $1/\lambda_B^{\pm}(n-q)$ is directly related to the ω -dependence of $\phi_{\pm}(\omega)$.

Finally, we compute the effect of the B meson LCDA shape on the branching ratio. In Fig. 10, we show the dependence of the branching ratio in the $[4m_{\mu}^2, 0.96]$ q^2 bin on λ_B and the shape parameter a for the three models. For given λ_B on the horizontal axis, the bands are obtained by varying a in its allowed range. In black, we also show the exponential model. Comparing with our previous results, we observe that the dependence on the shape is about as large as the dependence on the r_{LP} variation from the power-suppressed form factor, see Fig. 7. The conclusion is thus similar to the case of $B \rightarrow \gamma \ell \nu$ [20]. Once sufficient data is available, a correlated determination of λ_B together with the shape parameter $\hat{\sigma}_1$ (and, perhaps, others) should be performed. The important point is that the predicted branching fractions are highly sensitive to B meson LCDA input, even if not necessarily λ_B alone.

5 Conclusion

Motivated by the first search and upper limit [8] for the rare charged-current B decay to a four-lepton final state $\ell \bar{\nu}_{\ell} \ell^{(\prime)} \bar{\ell}^{(\prime)}$, this work considered the calculation of the decay amplitude with factorization methods. Combining methods previously applied to $B^- \rightarrow \ell^- \bar{\nu}_{\ell} \gamma$ [5] and $B_s \rightarrow \mu^+ \mu^- \gamma$

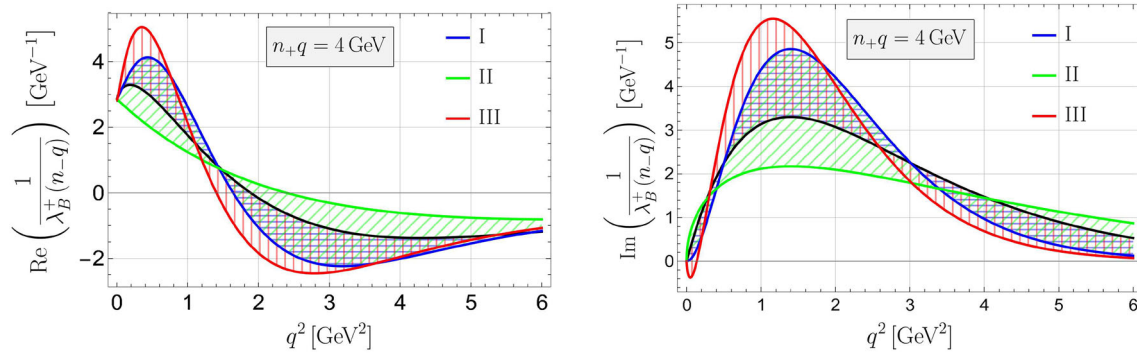


Fig. 8 The q^2 dependence of real (left) and imaginary (right) parts of $1/\lambda_B^+(n-q)$ at fixed $n+q = 4$ GeV for $\phi^{I,II,III}(\omega)$ in blue, green and red, respectively. The bands are obtained by varying the model parameter a within its range indicated in (4.4) for fixed $\lambda_B = 350$ MeV

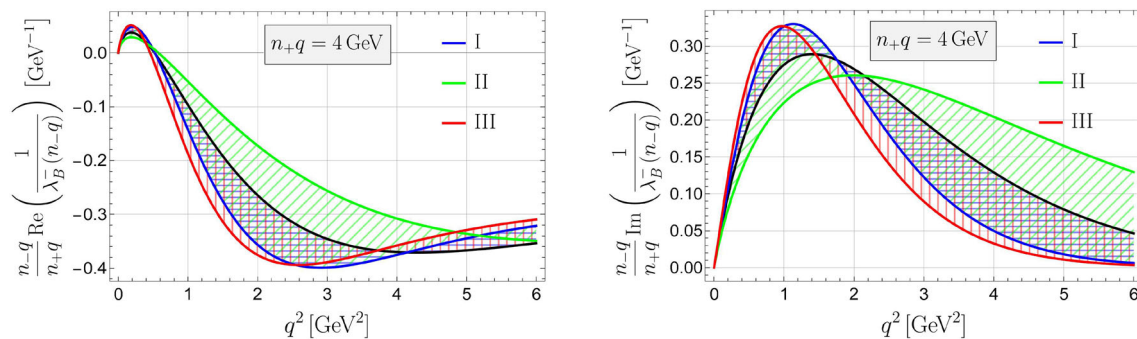


Fig. 9 As Fig. 8 but for $\frac{n-q}{n+q} \times 1/\lambda_B^-(n-q)$

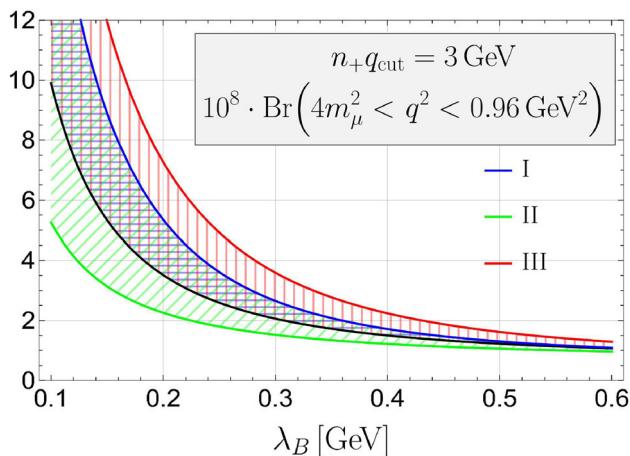


Fig. 10 Branching ratio (in 10^{-8}) of the $B^- \rightarrow \mu^- \mu^+ e^- \bar{\nu}_e$ decay mode in the $[4m_\mu^2, 0.96]$ q^2 bin for the three B LCDA models of (4.4) as a function of λ_B at scale 1.5 GeV. The bands are obtained by varying the model parameters within their allowed ranges. The solid black curve refers to the exponential model

[11], we obtain the $B \rightarrow \gamma^*$ form factors, which depend on the invariant masses of the two lepton pairs, in QCD factorization at next-to-leading order in α_s and leading power in an expansion in Λ_{QCD}/m_b , and to leading order in α_s at next-to-leading power. To this we added a simple Breit–Wigner parametrization of the ρ , ω intermediate resonances.

Although suppressed beyond next-to-leading power, the resonances dominate the spectrum in the $\ell^{(\prime)} \bar{\ell}^{(\prime)}$ invariant mass $\sqrt{q^2}$ locally, making the predictions more uncertain in this region than at large invariant mass or for $B^- \rightarrow \ell^- \bar{\nu}_\ell \gamma$. Quite generally it must be noted that the parametric counting that justifies the heavy-quark expansion is not well respected, as is evidenced by the large contribution of the longitudinal polarization state of the intermediate virtual photon.

Our calculations predict branching fractions of a few times 10^{-8} in the q^2 bin up to 1 GeV^2 , which are accessible to the LHC experiments. The branching fraction rapidly drops with increasing q^2 , reaching 10^{-9} in the bin $[1.5, 6]$ GeV^2 .

Confronting these results to measurements checks our understanding of Standard Model dynamics in these rare decays. An important further motivation for this investigation has been to explore the sensitivity of the decay rate to the inverse moment λ_B of the leading-twist B meson light-cone distribution amplitude. For non-vanishing q^2 the access to λ_B is less direct than in $B^- \rightarrow \ell^- \bar{\nu}_\ell \gamma$, and requires some knowledge of the shape of the LCDA as well. At large q^2 , the sensitivity disappears. We find these expectations confirmed in Fig. 7, which shows that λ_B is best determined from the small- q^2 bin. In this bin the sensitivity to λ_B is almost comparable to $B^- \rightarrow \ell^- \bar{\nu}_\ell \gamma$ when $\lambda_B < 200$ MeV, but less when it is larger. However, one should be aware that in this bin the resonance contribution is sizeable and there is unquan-

tified model dependence related to its interference with the factorization contribution. The q^2 bin above 1 GeV^2 can still yield useful bounds on λ_B , despite its weaker sensitivity. As for the case of $B \rightarrow \gamma \ell \nu$ [20], once sufficient data is available, a correlated determination of λ_B together with B meson LCDA shape parameters should be performed. Overall, we conclude that the four-lepton final state cannot fully replace the $B^- \rightarrow \ell^- \bar{\nu}_\ell \gamma$ mode to measure λ_B . However, given the current state of knowledge, any complementary experimental result on λ_B is worthwhile pursuing.

Note added

While this paper was being finalized, Ref. [31] appeared. We note the following important differences: (1) the third independent form factor, related to $F_{A\parallel}$, is missed, see Appendix A. (2) The q^2 distribution is computed without a cut on $n+q$, hence includes significant phase-space regions where the adopted QCD factorization treatment is not applicable. (3) The residual scale dependence of the leading-power form factor at NLO in the strong coupling is much larger than ours. Presumably this is because it is assumed (incorrectly) that the form of the exponential model is preserved by renormalization group evolution. (4) Only the region of small $q^2 < 1 \text{ GeV}^2$ is discussed. In this region our results are dominated locally by the Breit–Wigner parameterization of the ρ and ω resonances, whereas [31] adopts the QCD sum rule expression [32] for the power-suppressed form factor ξ , but in the time-like region. (5) For the case of identical lepton flavours, we present partially integrated branching fractions that correspond to experimental observables.

Acknowledgements We thank A. Khodjamirian, D. van Dyk and R. Zwicky for discussions. This research was funded in part by the Deutsche Forschungsgemeinschaft (DFG, German Research Foundation) – Project-ID 196253076-TRR 110 “Symmetries and the Emergence of Structure in QCD”.

Data Availability Statement This manuscript has associated data in a data repository. [Authors’ comment: All data generated or analysed during this study are included in this published article.]

Open Access This article is licensed under a Creative Commons Attribution 4.0 International License, which permits use, sharing, adaptation, distribution and reproduction in any medium or format, as long as you give appropriate credit to the original author(s) and the source, provide a link to the Creative Commons licence, and indicate if changes were made. The images or other third party material in this article are included in the article’s Creative Commons licence, unless indicated otherwise in a credit line to the material. If material is not included in the article’s Creative Commons licence and your intended use is not permitted by statutory regulation or exceeds the permitted use, you will need to obtain permission directly from the copyright holder. To view a copy of this licence, visit <http://creativecommons.org/licenses/by/4.0/>.
Funded by SCOAP³.

Appendix A: Decomposition of the hadronic tensor

Using Lorentz covariance only, the most general decomposition of the hadronic tensor $T^{\mu\nu}(p, q)$ defined in (2.2) contains six independent scalar form factors $F_{1\dots 6} = F_{1\dots 6}(k^2, q^2)$:

$$T^{\mu\nu} = F_1 g^{\mu\nu} + F_2 \epsilon^{\mu\nu\alpha\beta} k_\alpha q_\beta + F_3 k^\mu q^\nu + F_4 q^\mu k^\nu + F_5 k^\mu k^\nu + F_6 q^\mu q^\nu. \tag{A.1}$$

For $\gamma^* \rightarrow \bar{\ell}' \ell'$ and $W^* \rightarrow \ell \bar{\nu}_\ell$, the q^μ (k^ν) terms do not contribute to the decay amplitude if ℓ' (ℓ) is massless. The Ward identity $q_\mu T^{\mu\nu} = f_B (k + q)^\nu$ implies the relations

$$F_1 + F_3 q \cdot k + F_6 q^2 = f_B \quad \text{and} \quad F_4 q^2 + F_5 q \cdot k = f_B, \tag{A.2}$$

and hence reduces the number of independent form factors to four. We choose to eliminate F_3 and F_5 , and write

$$T^{\mu\nu} = F_1 g^{\mu\nu} + F_2 \epsilon^{\mu\nu\alpha\beta} k_\alpha q_\beta + \left(\frac{f_B - F_1 - q^2 F_6}{k \cdot q} \right) k^\mu q^\nu + F_4 q^\mu k^\nu + \left(\frac{f_B - q^2 F_4}{k \cdot q} \right) k^\mu k^\nu + F_6 q^\mu q^\nu. \tag{A.3}$$

Since we consider massless leptons we now can drop all terms in the second line, which leaves three independent form factors. The number of independent form factors can be associated with the number of independent polarization states of the virtual photon. Note that dropping $F_{4,5,6}$ in (A.1) before applying the Ward identity would lead to the omission of the F_6 term in the coefficient of the $k^\mu q^\nu$ term in (A.3), and to the wrong conclusion (since F_6 does not vanish) that there are only two independent form factors $F_{1,2}$ for massless leptons.⁶ It is straightforward to work out the relations between the form factors $F_{1,2,6}$ and $F_{A\perp, V, A\parallel}$ used in the main text.

Appendix B: Angular distribution

For non-identical leptons, we find that the full five-fold differential branching fraction

$$\frac{d^5 \text{Br} (B^- \rightarrow \ell \bar{\nu}_\ell \ell' \bar{\ell}')}{dq^2 dk^2 d \cos \theta_\gamma d \cos \theta_W d\phi} = \frac{\tau_B G_F^2 |V_{ub}|^2 \alpha_{\text{em}}^2 \sqrt{\lambda}}{2^{12} \pi^4 m_B^5} \frac{1}{q^4} \sqrt{1 - \frac{4m_{\ell'}^2}{q^2}} \times \left(1 - \frac{m_\ell^2}{k^2} \right) f(q^2, k^2, \Omega), \tag{B.1}$$

⁶ Since F_6 is multiplied by q^2 , this conclusion is correct for the $B \rightarrow \gamma$ form factors.

with $\Omega = (\theta_\gamma, \theta_W, \phi)$, assuming vanishing lepton masses, can be expressed in terms of nine independent angular coefficient functions $K_i = K_i(k^2, q^2)$, $i = 1 \dots 9$, as follows:

$$\begin{aligned} f(q^2, k^2, \Omega) &= K_1 \sin^2 \theta_W \sin^2 \theta_\gamma + K_2 (1 + \cos^2 \theta_W) \\ &\times (1 + \cos^2 \theta_\gamma) + K_3 \sin^2 \theta_W \sin^2 \theta_\gamma \sin^2 \phi + K_4 \cos \theta_W \\ &\times (1 + \cos^2 \theta_\gamma) + (K_5 + K_6 \cos \theta_W) \sin \theta_W \sin \theta_\gamma \cos \theta_\gamma \sin \phi \\ &+ (K_7 + K_8 \cos \theta_W) \sin \theta_W \sin \theta_\gamma \cos \theta_\gamma \cos \phi \\ &+ K_9 \sin^2 \theta_W \sin^2 \theta_\gamma \cos \phi \sin \phi. \end{aligned} \quad (\text{B.2})$$

Our definition of the helicity angles corresponds to the one in [33] (with the replacements $\theta_\Lambda^{[33]} \rightarrow \theta_\gamma$, $\theta_\ell^{[33]} \rightarrow \theta_W$ and $\phi^{[33]} \rightarrow \phi$), i.e. θ_W is the angle between \vec{p}_ℓ and the z axis in the rest frame of the $\ell\bar{\nu}_\ell$ system, θ_γ is the angle between \vec{q}_1 and the z axis in the dilepton rest frame, and ϕ is the relative angle between the decay planes. Introducing $f_{A\parallel} = \lambda F_{A\parallel}$, $f_V = 2\sqrt{k^2 q^2} \lambda F_V$, and $f_{A\perp} = 2\sqrt{k^2 q^2} (m_B^2 - k^2 + q^2) F_{A\perp}$ uniquely determines the kinematic functions that multiply the form factors, and we find:

$$K_1 = \frac{1}{4} (|f_{A\perp}|^2 - |f_V|^2 + 2|f_{A\parallel}|^2) \quad (\text{B.3})$$

$$K_2 = \frac{1}{4} (|f_{A\perp}|^2 + |f_V|^2) \quad (\text{B.4})$$

$$K_3 = -\frac{1}{2} (|f_{A\perp}|^2 - |f_V|^2) \quad (\text{B.5})$$

$$K_9 = -\text{Im}(f_{A\perp} f_V^*) \quad (\text{B.6})$$

$$K_4 = -\text{Re}(f_{A\perp} f_V^*) \quad (\text{B.7})$$

$$K_6 = -\text{Im}(f_{A\parallel} f_V^*) \quad (\text{B.8})$$

$$K_7 = -\text{Re}(f_{A\parallel} f_V^*) \quad (\text{B.9})$$

$$K_5 = \text{Im}(f_{A\parallel} f_{A\perp}^*) \quad (\text{B.10})$$

$$K_8 = \text{Re}(f_{A\parallel} f_{A\perp}^*). \quad (\text{B.11})$$

References

- G.P. Korchemsky, D. Pirjol, T.-M. Yan, Radiative leptonic decays of B mesons in QCD. Phys. Rev. D **61**, 114510 (2000). <https://doi.org/10.1103/PhysRevD.61.114510>. arXiv:hep-ph/9911427
- S. Descotes-Genon, C. Sachrajda, Factorization, the light cone distribution amplitude of the B meson and the radiative decay $B \rightarrow \gamma \ell \nu_\ell$. Nucl. Phys. B **650**, 356–390 (2002). [https://doi.org/10.1016/S0550-3213\(02\)01066-0](https://doi.org/10.1016/S0550-3213(02)01066-0). arXiv:hep-ph/0209216
- E. Lunghi, D. Pirjol, D. Wyler, Factorization in leptonic radiative $B \rightarrow \gamma \ell \nu$ decays. Nucl. Phys. B **649**, 349–364 (2003). [https://doi.org/10.1016/S0550-3213\(02\)01032-5](https://doi.org/10.1016/S0550-3213(02)01032-5). arXiv:hep-ph/0210091
- S. Bosch, R. Hill, B. Lange, M. Neubert, Factorization and Sudakov resummation in leptonic radiative B decay. Phys. Rev. D **67**, 094014 (2003). <https://doi.org/10.1103/PhysRevD.67.094014>. arXiv:hep-ph/0301123
- M. Beneke, J. Rohrwild, B meson distribution amplitude from $B \rightarrow \gamma \ell \nu$. Eur. Phys. J. C **71**, 1818 (2011). <https://doi.org/10.1140/epjc/s10052-011-1818-8>. arXiv:1110.3228
- M. Beneke, G. Buchalla, M. Neubert, C.T. Sachrajda, QCD factorization for $B \rightarrow \pi\pi$ decays: strong phases and CP violation in the heavy quark limit. Phys. Rev. Lett. **83**, 1914–1917 (1999). <https://doi.org/10.1103/PhysRevLett.83.1914>. arXiv:hep-ph/9905312
- Belle collaboration, M. Gelb et al., Search for the rare decay of $B^+ \rightarrow \ell^+ \nu_\ell \gamma$ with improved hadronic tagging. Phys. Rev. D **98**, 112016 (2018). <https://doi.org/10.1103/PhysRevD.98.112016>. arXiv:1810.12976
- LHCb collaboration, R. Aaij et al., Search for the rare decay $B^+ \rightarrow \mu^+ \mu^- \mu^+ \nu_\mu$. Eur. Phys. J. C **79**, 675 (2019). <https://doi.org/10.1140/epjc/s10052-019-7112-x>. arXiv:1812.06004
- A. Danilina, N. Nikitin, Four-leptonic decays of charged and neutral B mesons within the Standard Model. Phys. Atom. Nucl. **81**, 347–359 (2018). <https://doi.org/10.1134/S1063778818030092>
- A. Danilina, N. Nikitin, K. Toms, Decays of charged B-mesons into three charged leptons and a neutrino. Phys. Rev. D **101**, 096007 (2020). <https://doi.org/10.1103/PhysRevD.101.096007>. arXiv:1911.03670
- M. Beneke, C. Bobeth, Y.-M. Wang, $B_{d,s} \rightarrow \gamma \ell \bar{\ell}$ decay with an energetic photon. JHEP **12**, 148 (2020). [https://doi.org/10.1007/JHEP12\(2020\)148](https://doi.org/10.1007/JHEP12(2020)148). arXiv:2008.12494
- J. Albrecht, E. Stamou, R. Ziegler, R. Zwicky, Probing flavoured Axions in the Tail of $B_q \rightarrow \mu^+ \mu^-$. arXiv:1911.05018
- C.W. Bauer, S. Fleming, D. Pirjol, I.W. Stewart, An Effective field theory for collinear and soft gluons: heavy to light decays. Phys. Rev. D **63**, 114020 (2001). <https://doi.org/10.1103/PhysRevD.63.114020>. arXiv:hep-ph/0011336
- C.W. Bauer, D. Pirjol, I.W. Stewart, Soft collinear factorization in effective field theory. Phys. Rev. D **65**, 054022 (2002). <https://doi.org/10.1103/PhysRevD.65.054022>. arXiv:hep-ph/0109045
- M. Beneke, A. Chapovsky, M. Diehl, T. Feldmann, Soft collinear effective theory and heavy to light currents beyond leading power. Nucl. Phys. B **643**, 431–476 (2002). [https://doi.org/10.1016/S0550-3213\(02\)00687-9](https://doi.org/10.1016/S0550-3213(02)00687-9). arXiv:hep-ph/0206152
- M. Beneke, T. Feldmann, Multipole expanded soft collinear effective theory with non-abelian gauge symmetry. Phys. Lett. B **553**, 267–276 (2003). [https://doi.org/10.1016/S0370-2693\(02\)03204-5](https://doi.org/10.1016/S0370-2693(02)03204-5). arXiv:hep-ph/0211358
- Y.-M. Wang, Factorization and dispersion relations for radiative leptonic B decay. JHEP **09**, 159 (2016). [https://doi.org/10.1007/JHEP09\(2016\)159](https://doi.org/10.1007/JHEP09(2016)159). arXiv:1606.03080
- M. Beneke, T. Feldmann, Symmetry breaking corrections to heavy to light B meson form-factors at large recoil. Nucl. Phys. B **592**, 3–34 (2001). [https://doi.org/10.1016/S0550-3213\(00\)00585-X](https://doi.org/10.1016/S0550-3213(00)00585-X). arXiv:hep-ph/0008255
- M. Beneke, T. Feldmann, D. Seidel, Systematic approach to exclusive $B \rightarrow V l^+ l^-$, $V \gamma$ decays. Nucl. Phys. B **612**, 25–58 (2001). [https://doi.org/10.1016/S0550-3213\(01\)00366-2](https://doi.org/10.1016/S0550-3213(01)00366-2). arXiv:hep-ph/0106067
- M. Beneke, V. Braun, Y. Ji, Y.-B. Wei, Radiative leptonic decay $B \rightarrow \gamma \ell \nu_\ell$ with subleading power corrections. JHEP **07**, 154 (2018). [https://doi.org/10.1007/JHEP07\(2018\)154](https://doi.org/10.1007/JHEP07(2018)154). arXiv:1804.04962
- A. Bharucha, D.M. Straub, R. Zwicky, $B \rightarrow V \ell^+ \ell^-$ in the Standard Model from light-cone sum rules. JHEP **08**, 098 (2016). [https://doi.org/10.1007/JHEP08\(2016\)098](https://doi.org/10.1007/JHEP08(2016)098). arXiv:1503.05534
- HFLAV collaboration, Y.S. Amhis et al., Averages of b -hadron, c -hadron, and τ -lepton properties as of 2018. arXiv:1909.12524
- FLAVOUR LATTICE AVERAGING GROUP collaboration, S. Aoki et al., FLAG Review 2019: Flavour Lattice Averaging Group (FLAG). Eur. Phys. J. C **80**, 113 (2020). <https://doi.org/10.1140/epjc/s10052-019-7354-7>. arXiv:1902.08191

24. PARTICLE DATA GROUP collaboration, P. Zyla et al., Review of particle physics. PTEP **2020**, 083C01 (2020). <https://doi.org/10.1093/ptep/ptaa104>
25. ETM collaboration, A. Bussone et al., Mass of the b quark and B -meson decay constants from $N_f=2+1+1$ twisted-mass lattice QCD. Phys. Rev. D **93**, 114505 (2016). <https://doi.org/10.1103/PhysRevD.93.114505>. arXiv:1603.04306
26. A. Bazavov et al., B- and D-meson leptonic decay constants from four-flavor lattice QCD. Phys. Rev. D **98**, 074512 (2018). <https://doi.org/10.1103/PhysRevD.98.074512>. arXiv: 1712.09262
27. C. Hughes, C.T.H. Davies, C.J. Monahan, New methods for B meson decay constants and form factors from lattice NRQCD. Phys. Rev. D **97**, 054509 (2018). <https://doi.org/10.1103/PhysRevD.97.054509>. arXiv:1711.09981
28. HPQCD collaboration, R.J. Dowdall, C.T.H. Davies, R.R. Horgan, C.J. Monahan, J. Shigemitsu, B-meson decay constants from improved lattice nonrelativistic QCD with Physical u, d, s, and c Quarks. Phys. Rev. Lett. **110**, 222003 (2013). <https://doi.org/10.1103/PhysRevLett.110.222003>. arXiv: 1302.2644
29. FERMILAB LATTICE, MILC collaboration, J.A. Bailey et al., $|V_{ub}|$ from $B \rightarrow \pi \ell \nu$ decays and (2+1)-flavor lattice QCD. Phys. Rev. D **92**, 014024 (2015). <https://doi.org/10.1103/PhysRevD.92.014024>. arXiv:1503.07839
30. J.M. Flynn, T. Izubuchi, T. Kawanai, C. Lehner, A. Soni, R.S. Van de Water et al., $B \rightarrow \pi \ell \nu$ and $B_s \rightarrow K \ell \nu$ form factors and $|V_{ub}|$ from 2+1-flavor lattice QCD with domain-wall light quarks and relativistic heavy quarks. Phys. Rev. D **91**, 074510 (2015). <https://doi.org/10.1103/PhysRevD.91.074510>. arXiv:1501.05373
31. A. Bharucha, B. Kindra, N. Mahajan, Probing the structure of the B meson with $B \rightarrow \ell \ell' \nu$. arXiv:2102.03193
32. V.M. Braun, A. Khodjamirian, Soft contribution to $B \rightarrow \gamma \ell \nu_\ell$ and the B-meson distribution amplitude. Phys. Lett. B **718**, 1014–1019 (2013). <https://doi.org/10.1016/j.physletb.2012.11.047>. arXiv: 1210.4453
33. P. Böer, T. Feldmann, D. van Dyk, Angular Analysis of the Decay $\Lambda_b \rightarrow \Lambda(\rightarrow N\pi)\ell^+\ell^-$. JHEP **01**, 155 (2015). [https://doi.org/10.1007/JHEP01\(2015\)155](https://doi.org/10.1007/JHEP01(2015)155). arXiv:1410.2115